THE ASTROPHYSICAL JOURNAL, 344:135–145, 1989 September 1

EXCESS 10 MICRON EMISSION IN EXTRAGALACTIC NUCLEI

PAUL T. P. HO,[1] JEAN L. TURNER,[1,2] GIOVANNI G. FAZIO,[1] AND S. P. WILLNER[1]
Harvard-Smithsonian Center for Astrophysics
Received 1988 October 6; accepted 1989 February 1

ABSTRACT

Intense 10 μm emission has been mapped with 4″ resolution toward the nuclei of four nearby spiral galaxies: NGC 253, Maffei II, NGC 2903, and NGC 6946. In all four cases, the ratio of 10 μm to thermal radio emission is significantly higher than the ratio observed in Galactic H II regions. In addition, the 10 μm emission shows excellent spatial agreement with 6 cm radio continuum emission. This is surprising since the 10 μm emission is due to thermal dust emission, while the radio emission is predominantly nonthermal synchrotron emission. A new process that operates in galactic nuclei, but not in H II regions, may be responsible for much of the 10 μm emission. We propose that a population of small dust grains or large molecules heated by massive stars and supernova remnants (SNRs) may be responsible for an excess of 10 μm emission over the amount expected from radio free-free emission. The presence of an enhanced population of small dust grains in the nuclei of galaxies may result from dust destruction in shocks associated with the SNRs producing the radio emission, and the heating of these small grains may be via collisions with keV electrons associated with the SNRs.

Subject headings: galaxies: nuclei — infrared: sources — radiation mechanisms — radio sources: galaxies

I. INTRODUCTION

Both mid- and far-infrared studies (e.g., Rieke 1976; Rieke and Lebofsky 1978; Becklin *et al.* 1980; Telesco and Harper 1980; Telesco 1988) have shown that the nuclei of normal spiral galaxies are often bright at these wavelengths. The infrared emission is usually taken to indicate that vigorous star formation may be a common phenomenon in spiral nuclei. Rieke *et al.* (1980) have studied in detail two extremely bright nuclei, in M82 and NGC 253, and concluded that the infrared emission can be explained by a fairly recent burst of star formation. For many other galaxies, the infrared energy distributions and mass-to-light ratios are consistent with emission from dust heated by recently formed, early-type stars (Telesco and Harper 1980; Wynn-Williams 1988).

Star formation is closely linked to many observable properties of galaxies. For example, de Jong *et al.* (1985) have pointed out that there is a strong correlation between the far-infrared and radio flux densities. Since the far-infrared comes from dust heated primarily by newly formed stars while the radio emission is predominantly nonthermal synchrotron emission, these authors conclude that the good correlation between the two quantities suggests that young stars and the associated supernovae are the dominant source of relativistic electrons. These correlations are based on studies with low angular resolution and represent a global average over the disk of a galaxy.

This paper examines in more detail, and with high spatial resolution, the 10 μm emission from nuclear star-forming regions on 100 pc size scales. Although most of the energy emitted by newly formed stars eventually emerges in the far-infrared, making the far-infrared luminosity the best measure of recent star formation, 10 μm observations are useful since this is essentially the longest infrared wavelength currently observable with arcsecond resolution. Moreover, 10 μm emission can be used for high-resolution studies of distant galaxies beyond the reach of thermal radio continuum or Brackett line observations. Scoville *et al.* (1983), for example, have used 10 μm emission to infer star formation in Virgo spiral galaxies.

This work is part of a program to identify and calibrate reliable indicators of star formation in extragalactic nuclei. We have used the VLA to study the radio continuum emission from the nuclear regions of nearby spiral galaxies. Scaled-array observations at 2 and 6 cm wavelengths were used to obtain spectral index maps at 1″ resolution. Spatially separated regions of thermal and nonthermal emission can be identified (Turner and Ho 1983, 1989). We have also obtained near-infrared Brackett line observations of a number of these nuclei in order to measure the total number of ionizing photons, which can be compared with estimates based on radio continuum measurements (Beck, Turner, and Ho 1986; Turner, Ho, and Beck 1987).

In this paper, we compare the luminosities and spatial distributions of the 10 μm, thermal, and nonthermal radio structures in the nuclear star-forming regions of four nearby spiral galaxies. The observations are described and the data presented in § II. In § III we discuss the nature of the 10 μm emission and its relation to the radio continuum emission from the same region. The extended, intense 10 μm emission shows an excellent spatial correlation with the radio synchrotron emission. We propose in § IV a model in which a large population of collisionally heated small grains produce most of the 10 μm emission. Concentration of the small grains and the magnetic fields near shocks may naturally explain the spatial coincidences between the infrared and nonthermal radio emission.

II. OBSERVATIONS

The observations were made with the NASA Infrared Telescope Facility (IRTF) on Mauna Kea, Hawaii. The data were obtained on three sessions: 1983 August 18–20, 1984 January 16–18, and 1984 November 19–21. Because of terrible luck with weather, only 2.5 nights out of nine were usable. We used the IRTF 2–30 μm gallium-doped germanium bolometer,

[1] Visiting Astronomer at the Infrared Telescope Facility, which is operated by the University of Hawaii under contract from the National Aeronautics and Space Administration.

[2] Also University of California, Los Angeles.

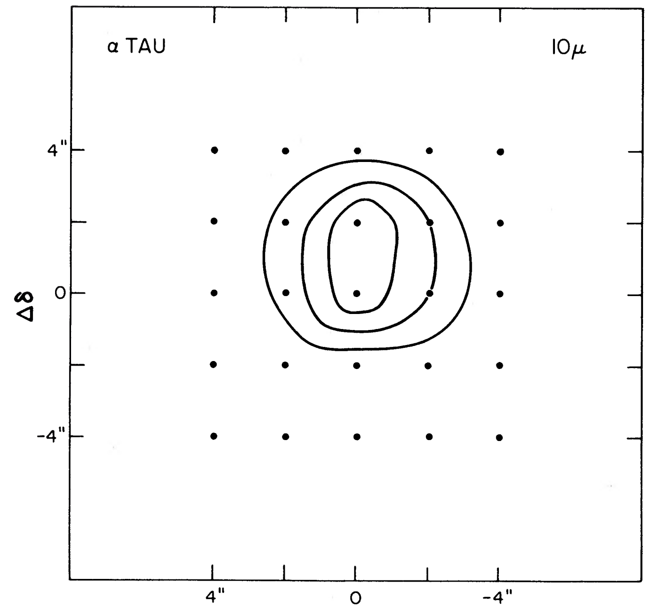

FIG. 1*a*

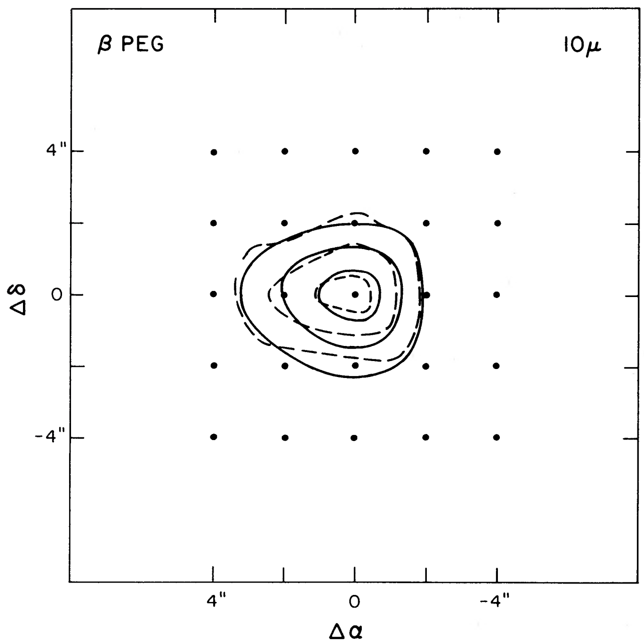

FIG. 1*b*

FIG. 1.—(*a*) 10 μm map of α Tau with 4″ aperture. The sampled data points as indicated are at 2″ steps. The contour levels are 25%, 50%, 75% of the peak flux of 620 Jy. (*b*) 10 μm map of β Peg with 4″ aperture. The sampled points and contour levels are as for α Tau. Peak flux of β Peg is 400 Jy.

which is cooled to liquid helium temperatures. The bolometer passband was defined by the standard *N* filter with $\Delta\lambda = 5.1$ μm centered at 10.1 μm or the *Q* filter with $\Delta\lambda = 9$ μm centered at 20 μm. We used a 2 mm aperture that yielded a 4″ beam. Typical integration times were 600 s, giving a 3 σ sensitivity of ∼0.06 Jy per beam. The telescope beam was mapped at 10 μm during 1987 January and November by observing the standard stars α Tau and β Peg (Figs. 1*a*, 1*b*). The beam responses were symmetrical, with FWHM of 3″–4″. Since these galactic nuclei are typically highly obscured in the visual, pointing was established by offsetting from nearby SAO stars. Absolute pointing was found to be better than 1″ by offsetting between SAO stars. We checked the pointing at 15 minute intervals by returning to the SAO stars. Tracking was found to be accurate to ∼1″. The infrared and optical beams were aligned on standard sources for various elevations. Sky subtraction was accomplished by chopping with respect to a reference position typically 30″–60″ away.

The principal uncertainty in the data is the statistical uncertainty due to detector and sky noise. Comparisons of the fluxes of various calibration sources at different elevations are consistent at the 10% level, and this is an indication of our absolute calibration uncertainty. Internal consistency within individual maps is less susceptible to systematic calibration problems and to variable or elevation-dependent atmospheric absorption, since data for individual galaxies were typically obtained close together in time and at nearly constant elevation angles. For these reasons, no corrections for atmospheric absorption have been applied. The small pointing errors of ∼1″ will also lead to uncertainties in relative intensities of ∼10%. This estimate was verified by repeated observations of nominal positions. Flux densities for the galaxies are referred to the adopted flux densities $S_{10\,\mu m}(\alpha$ Tau$) = 620$ Jy, $S_{10\,\mu m}(\beta$ Peg$) = 400$ Jy, and $S_{20\,\mu m}(\beta$ Peg$) = 110$ Jy.

Our sample of galaxies consists of NGC 253 [S(B)bc, 3.0 Mpc], Maffei II [S(B)b, 4.0 Mpc], NGC 2903 [S(B)bc, 6.2 Mpc], and NGC 6946 [S(B)cd, 10.8 Mpc]. Strong star-formation activity is present in each galaxy, while a weak active nucleus is present in NGC 253 (Turner and Ho 1985). These galaxies have strong CO line emission and large infrared luminosities and have been studied with high resolution in the radio continuum. Most importantly, they are close enough to permit detailed mapping at 10 μm.

The 10 μm maps of NGC 253, Maffei II, NGC 2903, and NGC 6946 are presented in Figures 2*a*–5*a*. The 10 μm maps are overlaid on $\lambda = 6$ cm, 1″ resolution radio continuum maps (Turner and Ho 1983, 1988) in Figures 2*b*–5*b*. In addition, we have obtained strip maps long the major axis of NGC 253 at 10 μm with 2″ resolution and at 20 μm with 4″ resolution. These strip scans are plotted in Figure 6 with the 10 μm data at 4″ resolution. The 10 μm maps of NGC 253 and NGC 2903 are in good agreement with the maps already published by Rieke and Low (1975) and Wynn-Williams and Becklin (1985).

III. DISCUSSION

There are two important results to be gleaned from these data. First, there is an excess in the ratio of 10 μm emission to radio free-free emission as compared to what is observed in Galactic H II regions. We shall discuss what we mean by a "10 μm excess" in the next section. Second, there is an excellent spatial correlation between the predominantly nonthermal radio emission and the 10 μm emission from warm dust. The spatial correlation is discussed in § III*b*. Given these results, we consider possible reasons why the mid-infrared emission in nuclear star-forming regions is different from that observed in Galactic H II regions.

a) *Excess* 10 μm *Emission*

The large 10 μm fluxes must be due to heated dust, as is the case for Galactic H II regions (e.g., Wynn-Williams and Becklin

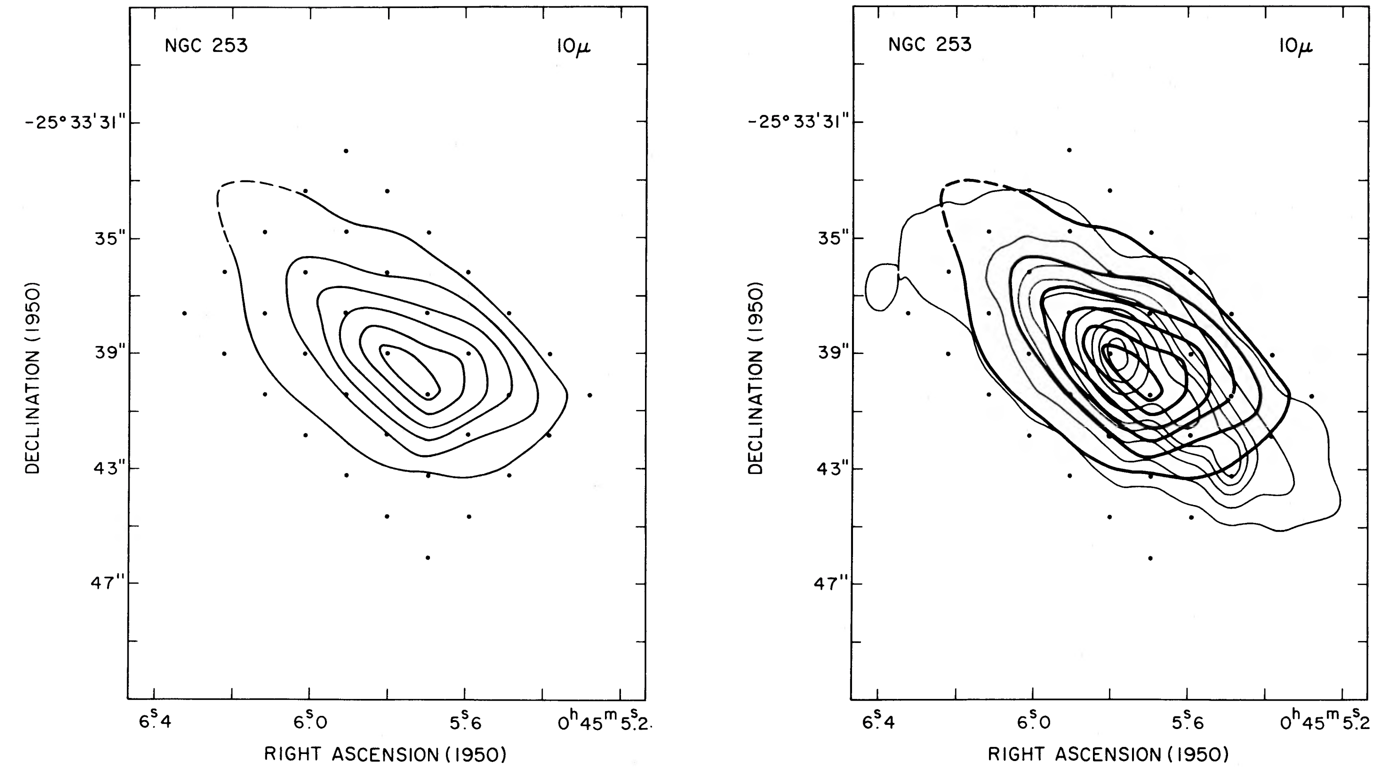

FIG. 2a FIG. 2b

FIG. 2.—(*a*) 10 μm map of NGC 253. Sampled data points are at half-beam steps of 2″ along the major and minor axis of the galaxy. The contour levels are 0.5, 1.0, 1.5, 2.0, 2.5, and 3.0 Jy per beam. (*b*) 10 μm map of NGC 253 superposed on 6 cm radio continuum map. The radio map is at 1″ resolution, and the radio contour levels are 4, 10, 20, 30, 40, 60, 100, 140, and 180 mJy per beam.

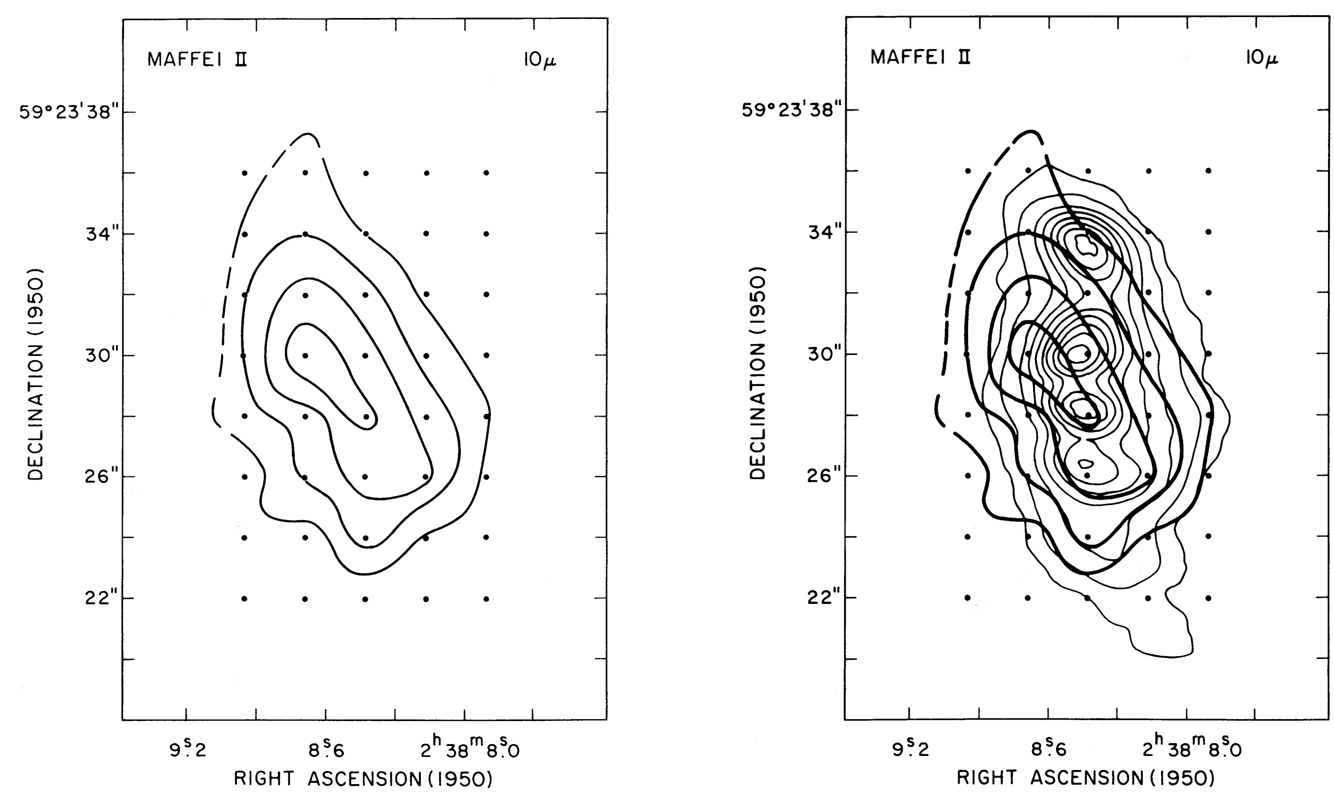

FIG. 3a FIG. 3b

FIG. 3.—(*a*) 10 μm map of Maffei II. Sampled data points are at 2″ steps in the R.A. and decl. directions. The contour levels are 0.10, 0.15, 0.20, and 0.25 Jy per beam. (*b*) 10 μm map of Maffei II superposed on 6 cm radio continuum map. The radio map is at 1″ resolution, with contour levels of 0.3, 0.6, 1.2, 1.8, 2.4, 3.0, 3.6, 4.2, 4.8, and 5.4 mJy per beam.

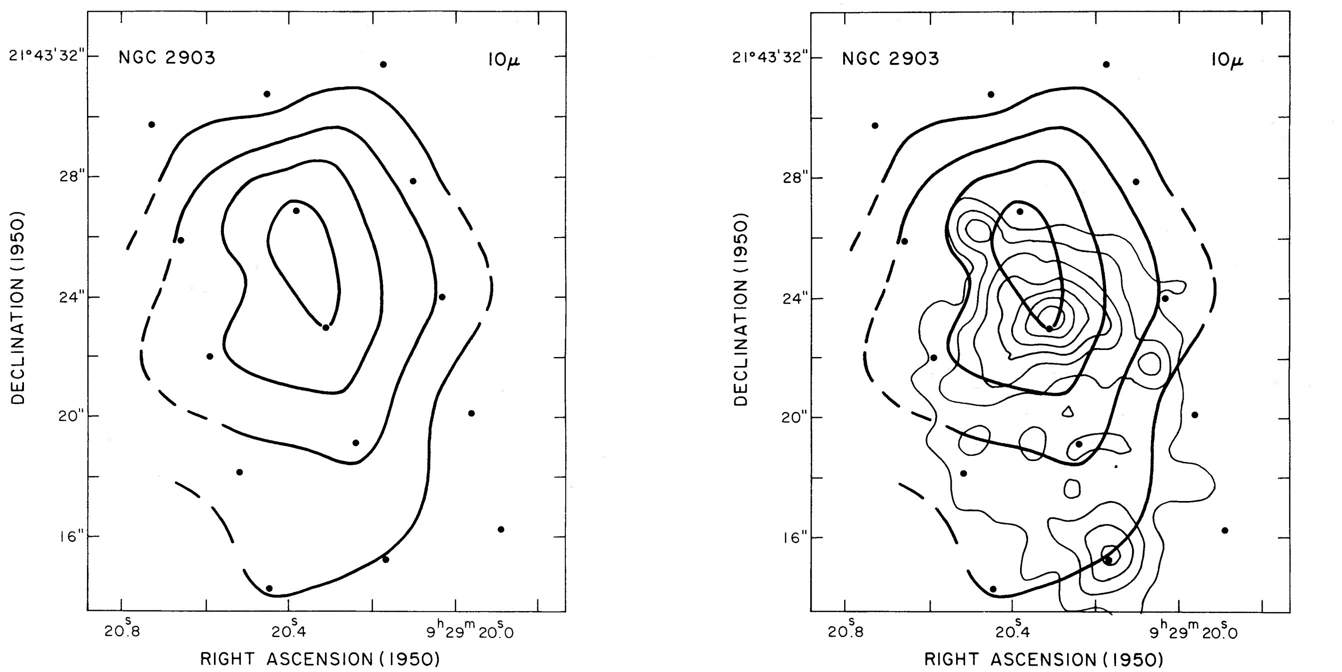

FIG. 4*a* FIG. 4*b*

FIG. 4.—(*a*) 10 μm map of NGC 2903. Sampled data points are at 2″ steps along the major and minor axis of the galaxy. The contour levels are 0.04, 0.07, 0.10, and 0.13 Jy per beam. (*b*) 10 μm map of NGC 2903 superposed on 6 cm radio continuum map. The radio map is at 1″ resolution, with contour levels of 0.2, 0.4, 0.6, 0.8, 1.0, 1.2, and 1.4 mJy per beam.

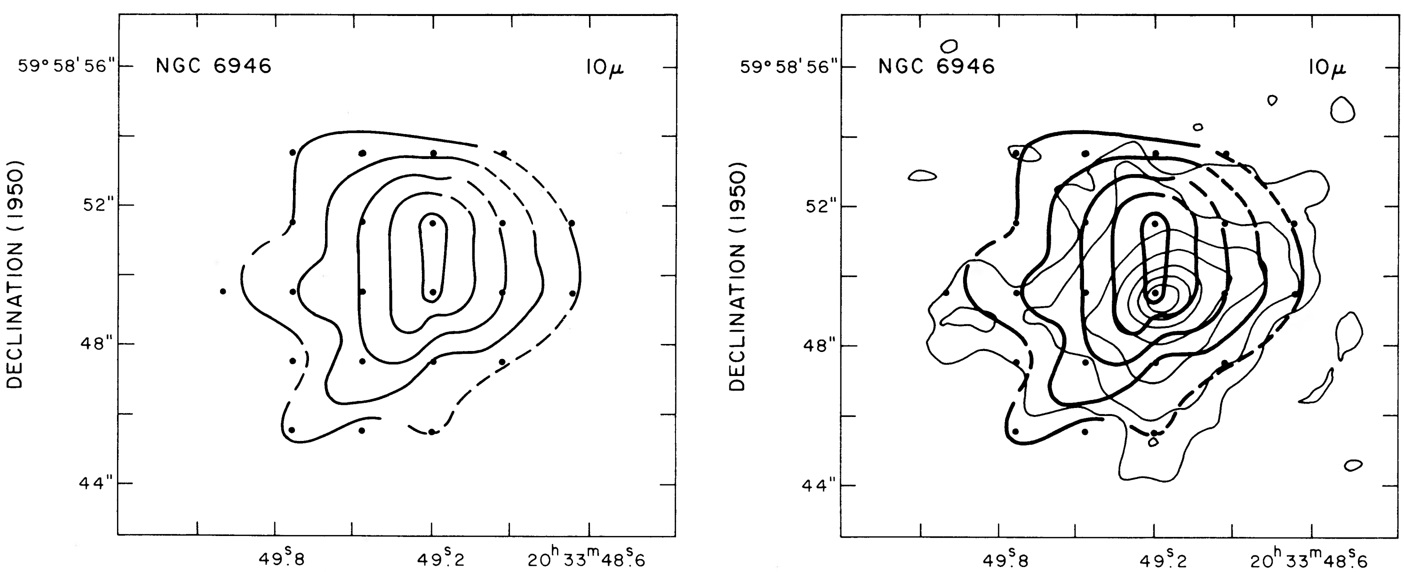

FIG. 5*a* FIG. 5*b*

FIG. 5.—(*a*) 10 μm map of NGC 6946. Sampled data points are at 2″ steps in the R.A. and decl. directions. The contour levels are 0.1, 0.2, 0.3, 0.4, and 0.5 Jy per beam. (*b*) 10 μm map of NGC 6946 superposed on 6 cm radio continuum map. The radio map is at 1″ resolution, with contour levels of 0.15, 0.30, 0.75, 1.5, 3.0, 4.5, and 6.0 mJy per beam.

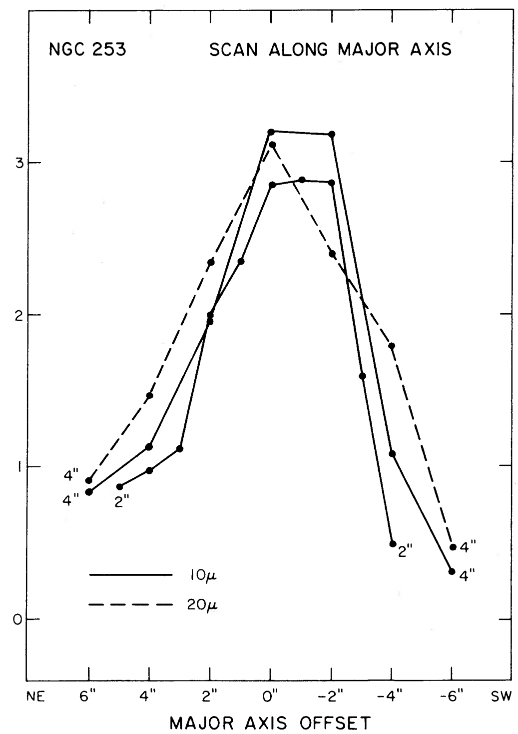

FIG. 6.—Strip maps along the major axis of NGC 253. The solid lines are scans at 10 μm. The dashed line is a scan at 20 μm. The aperture used in each scan is indicated. In order to compare the scans as a function of distance along the major axis, we have multiplied the 20 μm scan by a factor of 0.25, and the 10 μm scan at 2″ resolution by a factor of 1.5. Note that the flux ratio at 10 μm between the 4″ aperture and 2″ aperture is close to 2. This is consistent with the 10 μm emission being unresolved in the minor axis direction. The increase in the 10 μm to 20 μm ratio at −2″ offset in the southwest direction is also significant.

1974). Thermal free-free radiation and nonthermal synchrotron emission at 10 μm are limited by the detected radio flux densities and the observed spectral indices ($S_\nu \propto \nu^\alpha$). Table 1 gives the observed radio and 10 μm flux densities integrated over the same area for each nucleus. The 10 μm flux density exceeds the radio emission by factors of 10–30, ruling out both synchrotron and free-free emission, since the radio spectral indices are negative ($-0.6 \rightarrow -1.0$) in this sample. Self-absorbed synchrotron sources that peak at 10 μm and are hidden at radio frequencies can probably be ruled out because of the spatially extended (~100 pc) nature of the emission and unusual energy density requirements.

The correlation between the 10 μm fluxes and the thermal free-free radio continuum fluxes in Galactic H II regions is well known (e.g., Thronson, Campbell, and Harvey 1978; Lebofsky *et al.*, 1978; Strom *et al.*, 1974). The 10 μm emission comes from dust grains that are hotter than those producing the far-infrared emission, and the heating source for these relatively hot grains is probably Lyα trapped within H II regions (e.g., Wynn-Williams and Becklin 1974). Thronson, Campbell, and Harvey found that the ratio of 10 μm to radio free-free flux density has approximately the same value in extragalactic H II regions as in the local Galaxy, $S_{10\,\mu m}/S^{th}_{5\,GHz} = 10 \pm 3$. (Thronson, Campbell, and Harvey used 11 cm flux densities; since optically thin free-free emission declines by only 6% between 2.7 and 4.9 GHz, we take $S^{th}_{2.7\,GHz} \cong S^{th}_{5\,GHz}$.) This ratio would be produced by Lyα heating with a dust temperature of 150–200 K. Scoville *et al.* (1983) adopt a theoretical ratio $S_{10\,\mu m}/S^{th}_{5\,GHz} = 20$ for grain temperatures in the range 200–300 K in their study of Virgo galaxies. These values are reexamined in the next section.

The ratios of 10 μm flux density to thermal radio flux density observed for our sample of galactic nuclei greatly exceed the values discussed above. If we were to adopt the Galactic ratio of $S_{10\,\mu m}/S^{th}_{5\,GHz}$, almost all of the 6 cm radio fluxes in each of the galactic nuclei in our sample would have to be thermal. However, this is inconsistent with the observed steep radio spectral indices ($\alpha \approx -0.7$), which indicate that the bulk of the radio emission is nonthermal synchrotron emission (Turner and Ho 1983). We estimate that $S_{10\,\mu m}/S^{th}_{5\,GHz} > 50$–100 in our sample. This discrepancy has been noted before by Rieke (1976) and more recently by Wynn-Williams and Becklin (1985). It is unlikely that the large ratio $S_{10\,\mu m}/S^{th}_{5\,GHz}$ is generally produced by suppression of the radio emission: although it is possible for the radio free-free emission to be suppressed in optically thick compact H II regions, infrared Brackett recombination line observations of galactic nuclei generally do not indicate a deficiency in radio free-free emission (Beck, Turner, and Ho 1986; Ho, Beck, and Turner 1988). Furthermore, the lifetime of H II regions dense enough to be optically thick is only ~10^4 yr, much shorter than the stellar evolution lifetimes, so one would expect in general that the radio emission is dominated by longer lived, optically thin H II regions.

b) Spatial Distribution of the 10 μm *Emission*

The 10 μm emission in the nuclei of the four galaxies is in each case extended with respect to the telescope beam (FWHM > 4″ in at least one direction). There is good overall spatial agreement between the 10 μm and the 6 cm radio continuum emission (Figs. 2–5). This result has been demonstrated before. In particular, the study of M82 by Rieke *et al.* (1980) and of M83 by Telesco (1988) show very striking correspon-

TABLE 1

OBSERVED PROPERTIES OF GALAXY SAMPLE

Parameter	NGC 253	Maffei 2	NGC 6946	NGC 2903
Hubble type	S(B)bc I	S(B)b II	S(B)cd I	S(B)bc I-II
Distance (Mpc)	3.0	4.0	10.8	6.2
L_{IR} ($L_\odot$)	2.2(10)[a]	2.7(9)[b]	8.8(9)[b]	1.8(9)[b]
$S_{6\,cm}$ (mJy)[c]	1250	70	34	17
$S_{6\,cm}$–thermal (mJy)[c]	125	20	4	2
$S_{10\,\mu m}$ (mJy)	6800	1060	1030	860

[a] Telesco and Harper 1980.
[b] Rickard and Harvey 1983.
[c] Turner and Ho 1983, 1989.

dences between the 10 μm and the 6 cm emission. For our present sample, we examine the data for a more quantitative comparison. To reduce the effects of ($\sim 1''$) pointing uncertainties in the 10 μm maps and the different angular resolutions of the infrared and radio maps, we have convolved the 6 cm maps to 4″ resolution and compared the radio fluxes and 10 μm flux densities point by point. These are shown in Figure 7, which demonstrates a good correlation in each case. However, the scatter at any flux density level is much greater than noise and cannot be accounted for by systematic effects such as pointing errors in the 10 μm maps. We suggest that the overall spatial correlation implies that the 10 μm and radio continuum emission indeed arise from essentially the same regions at the scale of $\lesssim 100$ pc. The large scatter, instead of a tight correlation, suggests that the local conditions must play an important role in determining the 10 μm to radio continuum flux ratio. We emphasize that the scatter in the correlations is very significant, because each correlation in Figure 7 represents positions where the 10 μm and the radio continuum have been observed with the same angular resolution. Thus, the $S_{10\,\mu\mathrm{m}}/S_{5\,\mathrm{GHz}}$ ratio varies by a very large factor at arcsecond scales, while the overall correlation is good averaged over large scales. We emphasize also that the radio emission is predominantly nonthermal, so that $S_{10\,\mu\mathrm{m}}/S^{\mathrm{th}}_{5\,\mathrm{GHz}} \gg S_{10\,\mu\mathrm{m}}/S_{5\,\mathrm{GHz}}$.

c) *Radiative Dust Heating*

i) *Equilibrium Heating*

We reexamine here the possible sources for heating dust to temperatures high enough for it to emit at 10 μm. From the observed high surface brightness of the 10 μm emission for our sample of galactic nuclei (4×10^2–10^4 MJy sr^{-1}), we can reject circumstellar dust shells around late-type stars (<2 MJy sr^{-1} in M31; Soifer *et al.* 1986), as well as infrared cirrus heated by the interstellar radiation field (<1 MJy sr^{-1}; Weiland *et al.* 1986; Low *et al.* 1984). Heating of dust within an H II region by trapped Lyα photons, and heating by direct absorption of ionizing photons as well as nonionizing photons are possible radiative sources that we consider here (e.g., Krishna Swamy and O'Dell 1968; Petrosian, Silk, and Field 1972).

The expected 10 μm fluxes from Lyα heating were discussed by Genzel *et al.* (1982). The total integrated flux available from absorbed Lyα photons is

$$S_{\mathrm{IR}} = 1.4 \times 10^{-61}\ \mathrm{ergs\ s^{-1}\ cm^{-2}} \times N_{\mathrm{Lyc}} f\left(\frac{h\nu_{\mathrm{Ly}\alpha}}{1.64 \times 10^{-11}\ \mathrm{ergs}}\right)\left(\frac{D}{\mathrm{Mpc}}\right)^{-2}, \quad (1)$$

where N_{Lyc} is the number of Lyman continuum photons per second, and f is the number of Lyα photons ultimately derived from each Lyman continuum photon. The proportion of the total dust emission that is radiated at any frequency can be estimated by assuming a power-law dust emissivity $Q_\lambda \propto \lambda^{-\beta}$:

$$\frac{S_\nu}{S_{\mathrm{IR}}} = A_\beta \left(\frac{hc}{k\lambda T_G}\right)^{4+\beta} \frac{\lambda/c}{e^{hc/k\lambda T_G} - 1}\ \mathrm{Hz}^{-1}, \quad (2)$$

where T_G is the dust temperature, $A_\beta = 1.54 \times 10^{-1}$, 4.02×10^{-2}, and 8.19×10^{-3} for $\beta = 0$, 1, and 2. Note that N_{Lyc} can be obtained from either infrared recombination lines or thermal radio free-free emission. In the latter case, we can write

$$S^{\mathrm{th}}_{5\,\mathrm{GHz}} = 1.1\ \mathrm{mJy}\left(\frac{N_{\mathrm{Lyc}}}{10^{50}\ \mathrm{s}^{-1}}\right)\left(\frac{D}{\mathrm{Mpc}}\right)^{-2}\left(\frac{\nu}{4.9\ \mathrm{GHz}}\right)^{-0.1} \times \left(\frac{T_e}{10^4\ \mathrm{K}}\right)^{-0.35}\left(\frac{a}{0.994}\right)\left[\frac{\alpha^{(2)}}{2.616 \times 10^{-13}}\right]^{-1}, \quad (3)$$

where the correction factor a (Mezger and Henderson 1967) and the recombination coefficient $\alpha^{(2)}$ are weakly dependent on the electron temperature T_e. (The dependence of $S^{\mathrm{th}}_{5\,\mathrm{GHz}}$ on T_e is weak. If $T_e = 8000$ K, $S^{\mathrm{th}}_{5\,\mathrm{GHz}}$ decreases by $<10\%$.) Equation (1) then becomes

$$S_{\mathrm{IR}} = 1.2 \times 10^{-11}\ \mathrm{ergs\ s^{-1}\ cm^{-2}}\, f\left(\frac{S^{\mathrm{th}}_{5\,\mathrm{GHz}}}{\mathrm{mJy}}\right)\left(\frac{\nu}{4.9\ \mathrm{GHz}}\right)^{0.1}, \quad (4)$$

where we suppress the explicit dependence on T_e. Thus, $S_{10\,\mu\mathrm{m}}/S^{\mathrm{th}}_{5\,\mathrm{GHz}}$ can be derived from equations (2) and (4). Table 2 gives values derived for various grain temperatures and emissivity indices. Genzel *et al.* (1982) and Scoville *et al.* (1983) assume $\beta = 0$ for the dust emissivity, but numerous authors have noted that the emissivity is wavelength dependent (e.g., Mezger, Smith, and Churchwell 1974; Aannestad 1978; Scoville and Kwan 1976). Table 2 shows that for grain temperatures $T_G = 200$–500 K, $S_{10\,\mu\mathrm{m}}/S^{\mathrm{th}}_{5\,\mathrm{GHz}}$ is not very sensitive to the emissivity index or grain temperature because 10 μm is near the peak of the spectrum at those dust temperatures. For $T_G < 200$ K, corrections to $S_{10\,\mu\mathrm{m}}/S^{\mathrm{th}}_{5\,\mathrm{GHz}}$ due to the emissivity index can be substantial, but such cool grains do not radiate significantly at 10 μm. We conclude that dust heated by Lyα will radiate such that $S_{10\,\mu\mathrm{m}}/S^{\mathrm{th}}_{5\,\mathrm{GHz}} \leq 35$. It seems impossible to achieve a larger ratio of 10 μm to thermal radio emission if dust heating is solely via Lyα photons.

Direct absorption of stellar photons by dust has been considered by Petrosian, Silk, and Field (1972). They found that this contribution was necessary to explain the far-infrared luminosities of Galactic H II regions. Longward of the Lyman continuum limit, calculations show that, in our Galaxy, dust opacity in the vicinity of young stars is sufficient to absorb all of the stellar photons (Ho and Haschick 1981). The existence of 10 μm sources in the Galaxy that are "radio-weak" has been noted by Thronson, Campbell, and Harvey (1978). These authors suggested that dust heating in these cases is by low-ionization sources. For a cluster of OB stars, the later spectral types can contribute significant amounts of luminosity but little ionization. We estimate that for a Miller and Scalo (1979) initial mass function, the proportion of the total luminosity longward of the Lyman continuum limit is greater than 90% even for a lower mass cutoff of 20 $M_\odot$. An increase by a factor of 10 for $S_{\mathrm{IR}}/N_{\mathrm{Lyc}}$, over the value expected for pure Lyα heating, thus seems likely for clusters of stars. In the context of

TABLE 2

RATIO OF 10 MICRON TO THERMAL RADIO FLUX DENSITY

T_G (K)	$S_{10\,\mu\mathrm{m}}/S^{\mathrm{th}}_{5\,\mathrm{GHz}}$		
	$Q_\lambda \propto \lambda^0$	$Q_\lambda \propto \lambda^{-1}$	$Q_\lambda \propto \lambda^{-2}$
50........	1.4(−6)	1.0(−5)	6.2(−5)
100........	1.5(−1)	5.7(−1)	1.7(0)
150........	3.7(0)	9.0(0)	1.8(1)
200........	1.3(1)	2.4(1)	3.5(1)
300........	2.8(1)	3.5(1)	3.4(1)
400........	3.0(1)	2.8(1)	2.1(1)
500........	2.6(1)	1.9(1)	1.1(1)

1989ApJ...344..135H

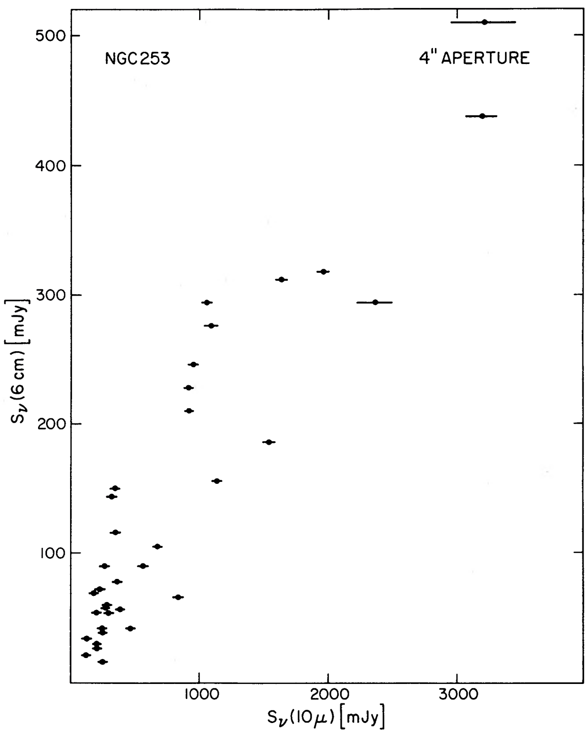

FIG. 7*a*

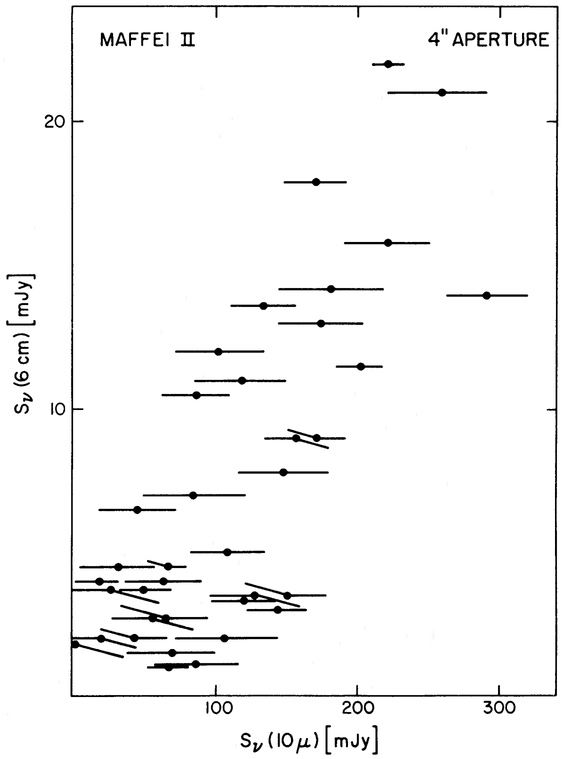

FIG. 7*b*

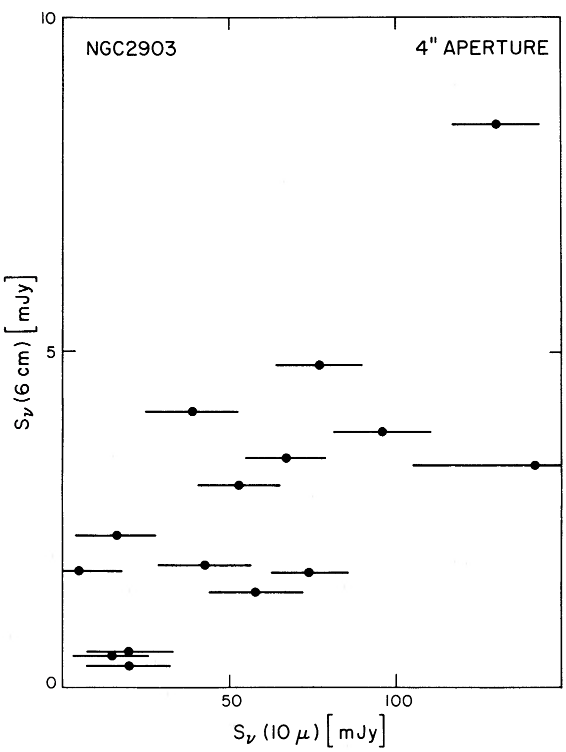

FIG. 7*c*

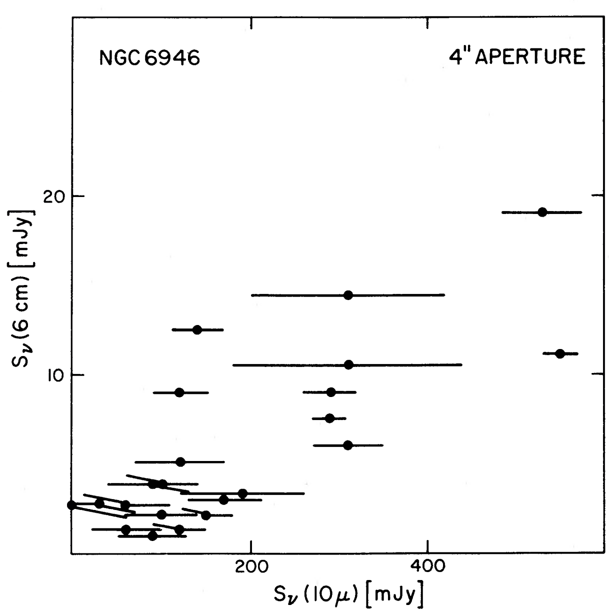

FIG. 7*d*

FIG. 7.—Correlation of 10 μm fluxes with 6 cm radio continuum fluxes. For this correlation, the radio continuum maps in Figs. 2–5 have been convolved with a Gaussian beam of FWHM of 4″. Fluxes are then compared point to point. (*a*) NGC 253, (*b*) Maffei II, (*c*) NGC 2903, (*d*) NGC 6946. Note that the bulk of the radio continuum flux is nonthermal, so that $S_{10\,\mu m}/S^{th}_{5\,GHz} \gg S_{10\,\mu m}/S_{5\,GHz}$.

starburst models (e.g., Rieke *et al.* 1980; Telesco and Gatley 1984), further evolution and a later age could be proposed in order to reduce even further the relative amount of ionizing flux.

While direct heating by stellar radiation is likely to dominate the far-infrared luminosity from these starburst regions, it is difficult to attain grain temperatures high enough to give significant emission at 10 μm. Both the ratio of *IRAS* 25 μm to 12 μm fluxes, and our own 20 μm and 10 μm flux measurements for NGC 253, imply a mid-infrared color temperature $\gtrsim$150 K. Such high-equilibrium dust temperatures can be attained only within 0.1 pc of OB stars (Scoville and Kwan 1976), and even smaller distances are required for less luminous stars. The spatially extended 10 μm emission (see Figs. 2–5) therefore requires that the OB stars must also be spatially distributed on the same scale of $\sim$200 pc. In addition, the associated H II regions might be compact and dense enough to be optically thick, suppressing the radio continuum emission, and thereby increasing the $S_{10\,\mu\mathrm{m}}/S^{\mathrm{th}}_{5\,\mathrm{GHz}}$ ratio.

Direct dust absorption of ionizing photons in compact H II regions could explain both the high dust temperature and the lack of radio continuum emission. However, the associated compact H II regions will expand at sound speeds ($\sim$10 km s^{-1}), so that this stage of emission will be brief ($\lesssim 10^4$ yr) and relatively rare. Another problem is the survival of grains within H II regions; there is some evidence that dust may be depleted within Galactic H II regions (Gillett *et al.* 1975; Willner 1977; Ho and Haschick 1981). Finally, in this model, the 10 μm emission is due to dust heated by compact H II regions which emit weakly in the radio, while the strong nonthermal radio emission must be provided by SNRs. The good spatial correlation between the hot dust and the SNR (see Figs. 2–5) implies a stringent constraint on the spatial distribution and evolution of two components with different ages.

ii) *Stochastic Radiative Heating of Small Dust Grains*

One possibility for relieving the requirement that grains be located very near the heating sources is to postulate a population of very small grains. Greenberg and Hong (1974) and Purcell (1976) have pointed out that if the grains are sufficiently small ($<$0.005 μm), the absorption of a single photon represents a substantial increase in the total energy of the grain. For a sufficiently small heat capacity, the dust temperature will be momentarily high. The effective temperature of the grain is then a time-dependent function of the incident photon energy and the emissivity of the grain. The important point is that since the heating process is due to single photons, the achieved temperature fluctuations are independent of the distance to the source of radiation. Wynn-Williams and Becklin (1985) have proposed that heating of small dust grains by visible or UV photons can account for excess 10 μm emission in extragalactic nuclei.

The existence of small grains and the effectiveness of transient heating have been established in Galactic reflection nebulae (Sellgren, Werner, and Dinerstein 1983; Sellgren 1984). Draine and Anderson (1985) and Désert, Boulanger, and Shore (1986) have calculated by independent methods the emergent infrared spectrum from small dust grains exposed to standard interstellar radiation fields. They find that the mid-infrared emission can be enhanced by factors greater than 10 if the distribution of grain sizes extends down to 0.0003 μm. Thus, enhanced emission at 10 μm and a high mid-infrared color temperature can be achieved, given a sufficiently large population of small grains, However, this picture leaves the spatial correlation of the infrared and radio emission unexplained.

d) Collisional Excitation of Small Grains

Collisional dust heating may provide the explanation for the observed correlation between the 6 cm nonthermal radio flux and the 10 μm emission. Collisional dust heating probably produces the observed 10 μm emission in Galactic supernova remnants (Braun *et al.*, 1986; Dwek *et al.* 1987). While collisional dust heating is relatively unimportant in Galactic star-forming regions, the large numbers of SNRs in starburst regions may make this a dominant heating mechanism. We shall discuss two collisional heating models: stochastic collisional heating (Désert, Boulanger, and Shore 1986; Dwek 1986), and equilibrium heating of dust behind shocks (Draine 1981; Dwek 1987). In either case, heating of the grains is through collisions with hot ($\sim 10^6$–10^8 K) gas; we show that the density of keV electrons is consistent with the observed population of relativistic electrons that produce the synchrotron emission.

i) *Stochastic Collisional Excitation of Small Grains in Hot Gas*

Small grains may be stochastically heated by collisions with energetic electrons in a hot, X-ray emitting gas (Dwek 1986). For a 10^7 K tenuous (10 cm^{-3}) plasma, as might be expected within a supernova cavity, Dwek has shown that the smallest grains will undergo collisionally induced temperature fluctuations. The dust temperature distribution peaks at a value lower than that from equilibrium calculations because of cooling between collisions, but the near-infrared radiation is enhanced due to contributions from the smaller grains. The difficulty in this model is whether the small dust grains will survive in a hot plasma. The estimate of lifetime for 0.0005 μm size grains is $\sim$500 yr under the assumed plasma conditions (Draine and Salpeter 1979; Dwek 1986). Both stochastic heating by electron collisions and stochastic heating by UV photons depend on the presence of small dust grains. For UV heating, however, the distance from the heating source to the dust is not important as long as sufficient grains are present and there is no intervening absorption. For the hot electrons, the dust grains must lie within the plasma. Hence, we expect a better spatial correlation between the 10 μm emission and the source of excitation in the latter case.

ii) *Collisional Equilibrium Heating of Small Grains in Shocks*

Another model that would produce an excess of 10 μm flux and the spatial agreement of the mid-infrared and synchrotron emission is the equilibrium collisional heating of grains in shocks. The shocks may be associated with the energetic outflows from an active nucleus or multiple supernovae. Either source is assumed to eject matter into the ambient interstellar medium at supersonic speeds. The resulting shocks betatron-accelerate and heat the gas; behind the shock, grains are heated by collisions with ions and electrons. A significant fraction of the total kinetic energy of the shock can appear in the mid-infrared (Draine 1981). Unlike the stochastic heating model, the equilibrium shock heating model is characterized by a single temperature and would require the hot dust component to be superposed on a cooler component in order to produce the observed infrared spectrum.

iii) *Radio Evidence for Hot Electrons*

The most direct way to explain the correlation of the 10 μm and synchrotron emission is if the same ultrarelativistic electrons that produce the radio emission collisionally heat the small grains. We estimate the electron energy by noting that a relativistic electron will radiate synchrotron emission predominantly at its critical frequency (Pacholczyk 1970),

$$\nu_C = \frac{3e}{4\pi m^3 c^5} B_\perp E^2 = 16.08 \text{ MHz} \left(\frac{B_\perp}{\mu\text{G}}\right)\left(\frac{E}{\text{GeV}}\right)^2 , \quad (5)$$

where $B_\perp$ is the perpendicular component of the magnetic field, and E is the energy of the electron. We can estimate $B_\perp$ from the equipartition value,

$$B_\perp \approx 190\ \mu\text{G}\left[\left(\frac{C_{12}}{2.8 \times 10^7}\right)\left(\frac{\theta}{1''}\right)^{-3}\left(\frac{D}{3\text{ Mpc}}\right)^{-1} \times \left(\frac{S_{\nu 0}}{10\text{ mJy}}\right)\left(\frac{0.3}{1+\alpha}\right)\left(\frac{\nu_0}{5\text{ GHz}}\right)^{0.7}\left(\frac{\nu_0}{100\text{ GHz}}\right)^{\alpha+0.7}\right]^{2/7} , \quad (6)$$

where C_{12} is a function of α (Pacholczyk 1970), $\alpha = -0.7$, and we assume an upper frequency cutoff of 100 GHz and equal energies in protons and electrons. The frequency ν_0 appears twice since we are assuming an upper frequency cutoff. Even the lowest energy synchrotron electrons that we can observe, radiating at the low-frequency cutoff of the ionosphere (~ 10 MHz), have energies on the order of 60 MeV.

Dwek (1987) gives the threshold energy for an electron to penetrate a grain, E^*. For a grain radius $\lesssim 0.005$ μm as required for stochastic heating, electrons will be stopped in the grain only for $E^* \lesssim 0.5$ keV. Therefore the relativistic electrons responsible for radio synchrotron emission will all penetrate the grains with negligible heating effects.

We may, however, infer the presence of keV electrons from the observed relativistic electron population, if a power-law distribution holds for electron energies down to the keV range. For the adopted values $\alpha \sim -0.7$, $S_{5\text{ GHz}} = 10$ mJy, and $\theta = 1''$, we obtain the density of electrons between 70 eV and 70 keV, $N_{E*} \sim 400$ cm^{-3}. This electron density is sufficiently high ($N_{E*} \gtrsim 1$ cm^{-3}) to heat the grains (Dwek 1986). The thermal free-free emission at radio wavelengths from these keV electrons will be small. However, N_{E*} depends strongly on spectral index; if $\alpha \sim -0.3$, $N_{E*} \sim 10^{-3}$ cm^{-3}. We note that the observed spectral index at radio wavelengths is steep, e.g., $\alpha < -0.7$ for both NGC 253 and NGC 6946 at arcsecond scales (Turner and Ho 1983). However, there is no direct information on α at keV energies, where ionization losses could drastically reduce the electron population.

Theoretical considerations also suggest the presence of keV electrons. Shock acceleration models do predict a power-law distribution in electron energy (Bell 1978*a*, *b*; Blandford and Ostriker 1978, 1980; Michel 1981); this power-law distribution is observed over many decades of energy in the Galaxy (Linsley 1980; Ginzberg and Syrovatskii 1964). In these models, suprathermal electrons in the tail of the thermal ($\sim$keV) electron distribution in the hot gas behind the shock are repeatedly accelerated by internally generated Alfvén wave/turbulent scattering back and forth across the shock, gaining energy at each pass. The final energy spectrum is a power law. Using this model, we can estimate the electron density as a function of energy for an encounter of a cloud of $n_H = 1$ cm^{-3} with a 10^4 km s^{-1} shock front (Bell 1978*b*); N_e (1 keV) ~ 10 cm^{-3} keV^{-1}, in good agreement with our estimate above.

There is also observational evidence that keV electrons exist in the nuclei of these galaxies. Electrons having energies of ~ 70 eV to ~ 1 keV correspond to thermal temperatures of 10^6–10^8 K. These temperatures are characteristic of the slowly cooling interiors of Galactic SNRs. Two galaxies in our sample, NGC 253 and NGC 2903, have been detected in the X-ray by the *Einstein Observatory* (Fabbiano, Trinchieri, and Macdonald 1984; Fabbiano and Trinchieri 1984). Both Fabbiano, Trinchieri, and Macdonald (1984) and Watson, Stanger, and Griffiths (1984) argue in favor of thermal bremsstrahlung and against nonthermal emission from ultrarelativistic electrons as the origin of the X-ray emission. Thus, electrons in the requisite energy range for stochastic heating (Dwek 1986) are probably present.

We conclude that although the ultrarelativistic electrons responsible for the radio emission do not interact with the dust grains, the associated lower energy electrons will. Theoretical considerations suggest that the presence of these lower energy electrons is required in order to produce the power-law distribution of relativistic electrons. The deduced densities of low-energy electrons are high enough to make collisional heating of dust plausible.

e) An Enhanced Population of Small Grains

The major question that we are trying to address is: why is the mid-infrared emission from nuclear starburst regions so different from that of Galactic H II regions? What is it about its position in a starburst that tells a grain to radiate more strongly in the mid-infrared? We have previously discussed dust heating mechanisms that may come to play in starburst regions and that might enhance mid-infrared emission over that expected for normal H II regions. But the grain population itself is likely to be affected by the proximity of large numbers of SNRs and shocks.

The action of shocks on dust grains is complicated (Draine and Salpeter 1979). The destruction of the larger grains in shocks is likely to increase the number of smaller grains (Seab 1987; McKee *et al.* 1987). The enhanced mid-infrared emission seen in starbursts may be the result of a grain size distribution that is skewed considerably to the smallward from the normal Mathis-Rumpl-Nordsieck (1977) grain size distribution. The skewing may be due to the extremely high density of SNRs and a correspondingly high rate of shock processing of grains.

There is observational support for small grains in the 8–13 μm spectra of nuclear star-forming regions (Roche 1986; Roche and Aitken 1985; Roche *et al.* 1984). Like Galactic H II regions, extragalactic starburst regions have strong, narrow infrared features in the 8–13 μm band. These features are likely to be associated with small grains (Sellgren 1984), and one suggested identification is polyatomic aromatic hydrocarbons (Léger and Puget 1984), likely to be formed in shocks (Omont 1986). Roche and Aitken find that the 7.7, 8.3, and 11.25 μm features dominate many of the 10 μm spectra in star-forming galaxies. If the identification of these features is correct, perhaps much of the 10 μm excess is produced by the smallest grains, whose numbers have been enhanced by the high density of SNR shocks.

f) Infrared Emission from Galactic SNRs

Shock heating of dust has been observed in Galactic SNRs. Braun and Strom (1986) report *IRAS* observations of dust in the Cygnus Loop. The observed dust emission is clearly associated with and inside the remnant. Although the 12 μm *IRAS* fluxes are uncertain in this case, the nominal ratio $S_{25\ \mu m}/S_{12\ \mu m}$ is ~ 4, similar to our sample of galactic nuclei. The shell-like morphology of the infrared emission suggests that the emission originates in the hot gas behind the shock (Draine 1981). Analysis of *IRAS* observations of the Cassiopeia A remnant by Dwek *et al.* (1987) supports shock heating of very small grains. The observed surface brightness at 12 μm is only 0.02 MJy sr^{-1} for an old SNR such as Cygnus Loop (Braun and Strom 1986) but is $\sim$16 MJy sr^{-1} for a younger remnant such as Cassiopeia A (Braun *et al.* 1986). The intensities we see in our sample of galaxies are $\sim 10^3$–10^4 MJy sr^{-1}. The dust emission intensity scales as $n_H v_s^3$, where n_H is the density of the ambient gas ($\sim$2 cm^{-3} for Cas A), and v_s is the shock velocity (Draine 1981). We might expect much higher surface brightnesses in the nuclei of galaxies where gas densities may be higher by more than a factor of 100. The observed properties of the 10 μm emission may be explained by very young supernovae expanding into relatively dense gas (e.g., Wheeler, Mazurek, and Sivaramakrishnan 1980; Shull 1980).

The additional heating in the shock model explains the excess of 10 μm to thermal radio emission in the galactic nuclei as compared to the H II regions. It also explains the concentration of 10 μm emission toward the nucleus and the good correlation with synchrotron emission. Shocks from numerous supernovae or from an active nucleus are not likely to be found outside galactic nuclei. The model may also explain the large dispersion at arcsecond scales in the ratio of 10 μm emission and radio continuum emission as due to intrinsic differences in local properties such as cloud densities and magnetic fields and shock velocities.

The notion that supernovae may play a strong role in the mid-infrared emission is interesting in light of the strong correlation seen between the total far-infrared flux and the total radio flux as discussed by de Jong *et al.* (1985). The latter results represent averages over large scales, where both types of emission may be good estimators of the total number of young OB stars. The present results suggest that even at small scales, the dust component already interacts noticeably with supernovae.

IV. CONCLUSIONS

We observe intense 10 μm continuum emission in the nuclei of four galaxies. The spatial distribution of 10 μm emission is remarkably like that of the nonthermal radio emission. Detailed comparisons show that although the overall correlation is good, there is a large dispersion in the $S_{10\,\mu m}/S_{5\,GHz}$ ratio at arcsecond scales. There is insufficient thermal radio emission, and hence ionization flux, to account for the 10 μm emission by Lyα heating or by other processes prevalent in Galactic or extragalactic H II regions. The galactic nuclei thus require the presence of some additional mechanism that produces 10 μm emission. This process must be consistent with the good spatial correlation between the infrared and radio emission, while allowing for a sizable dispersion.

One possible model is that the dust is radiatively heated by clusters of stars extending to low enough masses to provide a significant amount of nonionizing flux. This can then explain a high ratio for $S_{10\,\mu m}/S_{5\,GHz}^{th}$. However, this model requires that dust be concentrated very close to the heating stars in order to obtain a high grain temperature. If these conditions are indeed present in the galactic nuclei, there is no obvious reason that they should not be present in other H II regions. Moreover, this model does not explain the excellent spatial agreement between the 10 μm and the nonthermal 6 cm emission, found in these studies as well as others reported in the literature.

A second model is that the 10 μm emission results from collisional heating of dust in shocks. The shocks might originate in supersonic outflows from an active nucleus or, more likely for these galaxies, from many nuclear supernovae. These outflows shock the interstellar medium immediately outside of the nucleus. The shocks accelerate electrons, concentrate the interstellar magnetic field, and form small dust grains. The highest energy electrons and the magnetic fields produce synchrotron radio emission, while the lower energy electrons heat dust grains. The small dust grains formed in the shock are transiently heated by individual electron collisions to temperatures high enough to radiate at 10 μm. If the shock heating model is valid, strong 10 μm emission directly indicates the presence of energetic particles and dust grains. If the shocks are entirely due to SNRs, a connection between 10 μm emission and strong star-formation activities would be established. However, at least for NGC 253, there is the possibility that an active nucleus may be responsible for the nonthermal radio disk. Strong 10 μm dust emission, especially as an excess well above Lyα heating, may not uniquely indicate star formation, but may be a product of an active nucleus.

Whatever the heating mechanism, it is likely that the unusual mid-infrared emission that we see is due to an unusual population of dust grains. The fact that we observe many SNRs in the same region as this dust supports the idea that shock processing has heavily altered the grain size distribution, weighting it heavily toward the small grain-large molecule end. Mid-infrared spectroscopy will reveal more about this possibility.

We thank Mark Birkinshaw for many helpful suggestions and a careful reading of the manuscript. We also acknowledge enlightening discussions with Mike Jura. We thank the staff at IRTF and Alan Tokunaga for help and advice during our observations. Insightful comments and a rapid response from our anonymous referee are also gratefully acknowledged. P. T. P. H. is supported in part by NSF grant AST85-09907 and AST87-20759.

REFERENCES

Aannestad, P. A. 1978, *Ap. J.*, **220**, 538.
Beck, S. C., Turner, J. L., and Ho, P. T. P. 1986, *Ap. J.*, **309**, 70.
Becklin, E. E., Gatley, I., Matthews, K., Neugebauer, G., Sellgren, K., Werner, M. W., and Wynn-Williams, C. G. 1980, *Ap. J.*, **236**, 441.
Bell, A. R. 1978*a*, *M.N.R.A.S.*, **182**, 147.
———. 1978*b*, *M.N.R.A.S.*, **182**, 443.
Blandford, R. D., and Ostriker, J. P. 1978, *Ap. J.* (*Letters*), **221**, L29.
———. 1980, *Ap. J.*, **237**, 793.
Braun, R., and Strom, R. G. 1986, *Astr. Ap.*, **164**, 208.
Braun, R., Strom, R. G., van der Laan, H., and Greidanus, H. 1986, in *Light on Dark Matter*, ed. F. P. Israel (Dordrecht: Reidel), p. 155.
de Jong, T., Klein, U., Wielebinski, R., and Wunderlich, E. 1985, *Astr. Ap.*, **147**, L6.
Désert, F. X., Boulanger, F., and Shore, S. N. 1986, *Astr. Ap.*, **160**, 295.
Draine, B. T. 1981, *Ap. J.*, **245**, 880.
Draine, B. T., and Anderson, N. 1985, *Ap. J.*, **292**, 494.
Draine, B. T., and Salpeter, E. E. 1979, *Ap. J.*, **231**, 438.
Dwek, E. 1986, *Ap. J.*, **302**, 363.
———. 1987, *Ap. J.*, **322**, 812.
Dwek, E., Dinerstein, H. L., Gillett, F. C., Hauser, M. G., and Rice, W. L. 1987, *Ap. J.*, **315**, 571.
Fabbiano, G., and Trinchieri, G. 1984, *Ap. J.*, **286**, 491.

Fabbiano, G., Trinchieri, G., and Macdonald, A. 1984, *Ap. J.*, **284**, 65.
Genzel, R., Becklin, E. E., Wynn-Williams, C. G., Moran, J. M., Reid, M. J., Jaffe, D. T., and Downes, D. 1982, *Ap. J.*, **255**, 527.
Gillett, F. C., Forrest, W. J., Merrill, K. M., Capps, R. W., and Soifer, B. T. 1975, *Ap. J.*, **200**, 609.
Ginzburg, V. L., and Syrovatskii, S. I. 1964, *The Origin of Cosmic Rays* (Oxford: Pergamon).
Greenberg, J. M., and Hong, S. S. 1974, in *IAU Symposium 60, Galactic and Radio Astronomy*, ed. F. Kerr and S. C. Simonson III (Dordrecht: Reidel), p. 155.
Ho, P. T. P., Beck, S. C., and Turner, J. L. 1988, preprint.
Ho, P. T. P., and Haschick, A. D. 1981, *Ap. J.*, **248**, 622.
Krishna Swamy, K. S., and O'Dell, C. R. 1968, *Ap. J.* (*Letters*), **151**, L61.
Lebofsky, M. J., Sargent, D. G., Kleinmann, S. G., and Rieke, G. H. 1978, *Ap. J.*, **219**, 487.
Léger, A., and Puget, J. L. 1984, *Astr. Ap.*, **137**, L5.
Linsley, J. 1980, in *IAU Symposium 94, Origin of Cosmic Rays*, ed. G. Setti, G. Spada, and R. A. Wolfendale (Dordrecht: Reidel), p. 53.
Low, F. J., *et al.* 1984, *Ap. J.* (*Letters*), **278**, L19.
Mathis, J., Rumpl, W., and Nordsieck, K. H. 1977, *Ap. J.*, **217**, 425.
McKee, C. F., Hollenback, D. J., Seab, C. G., and Tielens, A. G. G. M. 1987, *Ap. J.*, **318**, 674.
Mezger, P. G., and Henderson, A. P. 1967, *Ap. J.*, **147**, 471.
Mezger, P. G., Smith, L. F., and Churchwell, E. 1974, *Astr. Ap.*, **32**, 269.
Michel, F. C. 1981, *Ap. J.*, **247**, 664.
Miller, G. M., and Scalo, J. M. 1979, *Ap. J. Suppl.*, **41**, 513.
Omont, A. 1986, in *Polycyclic Aromatic Hydrocarbons and Astrophysics*, ed. A. Léger, L. D'Hendecourt, and N. Boccara (Dordrecht: Reidel), p. 351.
Pacholczyk, A. G. 1970, *Radio Astrophysics* (San Francisco: Freeman).
Petrosian, V., Silk, J., and Field, G. B. 1972, *Ap. J.* (*Letters*), **177**, L69.
Purcell, E. M. 1976, *Ap. J.*, **206**, 685.
Rickard, L. J., and Harvey, P. M. 1983, *Ap. J.* (*Letters*), **268**, L7.
Rieke, G. H. 1976, *Ap. J.* (*Letters*), **206**, L15.
Rieke, G. H., and Lebofsky, M. J. 1978, *Ap. J.* (*Letters*), **220**, L37.
Rieke, G. H., Lebofsky, M. J., Thompson, R. I., Low, F. J., and Tokunaga, A. T. 1980, *Ap. J.*, **238**, 24.
Rieke, G. H., and Low, F. J. 1975, *Ap. J.*, **197**, 17.
Roche, P. F. 1986, in *Polycyclic Aromatic Hydrocarbons and Astrophysics*, ed. A. Léger, L. D'Hendecourt, and N. Boccara (Dordrecht: Reidel), p. 307.
Roche, P. F., and Aitken, D. K. 1985, *M.N.R.A.S.*, **213**, 789.
Roche, P. F., Aitken, D. K., Phillips, M. M., and Whitmore, B. 1984, *M.N.R.A.S.*, **207**, 35.
Scoville, N. Z., Becklin, E. E., Young, J. S., and Capps, R. W. 1983, *Ap. J.*, **271**, 512.
Scoville, N. Z., and Kwan, J. 1976, *Ap. J.*, **206**, 718.
Seab, C. G. 1987, in *Interstellar Processes*, Vol. **2**, ed. D. Hollenbach and H. Thronson (Dordrecht: Reidel), p. 397.
Sellgren, K. 1984, *Ap. J.*, **277**, 623.
Sellgren, K., Werner, M. W., and Dinerstein, H. L. 1983, *Ap. J.* (*Letters*), **271**, L13.
Shull, J. M. 1980, *Ap. J.*, **237**, 769.
Soifer, B. T., Rice, W. L., Mould, J. R., Gillett, F. C., Robinson, M. R., and Habing, H. J. 1986, *Ap. J.*, **304**, 651.
Strom, S. E., Strom, K. M., Grasdalen, G. L., and Capps, R. W. 1974, *Ap. J.* (*Letters*), **193**, L7.
Telesco, C. M. 1988, *Ann. Rev. Astr. Ap.*, **26**, 343.
Telesco, C. M., and Gatley, I. 1984, *Ap. J.*, **284**, 557.
Telesco, C. M., and Harper, D. A. 1980, *Ap. J.*, **235**, 392.
Thronson, H. A., Campbell, M. F., and Harvey, P. M. 1978, *A.J.*, **83**, 1581.
Turner, J. L., and Ho, P. T. P. 1983, *Ap. J.* (*Letters*), **268**, L79.
———. 1985, *Ap. J.* (*Letters*), **299**, L77.
———. 1989, in preparation.
Turner, J. L., Ho, P. T. P., and Beck, S. C. 1987, *Ap. J.*, **313**, 644.
Watson, M. G., Stanger, V., and Griffiths, R. E. 1984, *Ap. J.*, **286**, 144.
Weiland, J. L., Blitz, L., Dwek, E., Hauser, M. G., Magnani, L., and Rickard, L. J. 1986, *Ap. J.* (*Letters*), **306**, L101.
Wheeler, J. C., Mazurek, T. J., and Sivaramakrishnan, A. 1980, *Ap. J.*, **237**, 781.
Willner, S. P. 1977, *Ap. J.*, **214**, 706.
Wynn-Williams, C. G. 1988, in *IAU Symposium 115, Star Forming Regions*, ed. M. Peimbert and J. Jugaku (Dordrecht: Reidel), p. 587.
Wynn-Williams, C. G., and Becklin, E. E. 1974, *Pub. A.S.P.*, **86**, 5.
———. 1985, *Ap. J.*, **290**, 108.

GIOVANNI G. FAZIO, PAUL T. P. HO, and S. P. WILLNER: Harvard-Smithsonian Center for Astrophysics, 60 Garden Street, Cambridge, MA 02138

JEAN L. TURNER: Department of Astronomy, UCLA, Los Angeles, CA 90024